arXiv:hep-ph/0109122v2 16 Nov 2001

hep-ph/0109122
TU–629
KEK–TH–783
September 2001

Perturbative QCD Potential, Renormalon Cancellation and Phenomenological Potentials

S. Recksiegel[1] and Y. Sumino[2]

[1] Theory Group, KEK
Tsukuba, Ibaraki, 305-0801 Japan

[2] Department of Physics, Tohoku University
Sendai, 980-8578 Japan

Abstract

We examine the total energy $E_{\rm tot}(r) = 2m_{\rm pole} + V_{\rm QCD}(r)$ of the $b\bar{b}$ system within perturbative QCD up to $\mathcal{O}(\alpha_S^3)$. We extend a previous analysis by incorporating effects of the non-zero charm-quark mass in loops. We find that, once the renormalon cancellation is performed, $E_{\rm tot}(r)$ agrees well with typical phenomenological potentials for heavy quarkonia at distances $0.5~{\rm GeV}^{-1} \lesssim r \lesssim 3~{\rm GeV}^{-1}$. We also examine the perturbative predictions for $E_{\rm tot}(r)$ of other heavy quarkonium systems. Whenever stable predictions are obtained, they agree with each other up to an r-independent constant.

1 Introduction

Heavy quarkonium systems, such as bottomonium and charmonium, provide an important testing ground for theoretical studies on the dynamics of QCD boundstates. For decades, theoretical methods for investigating these systems have followed paths different from those used for studying the QED boundstates such as positronium or the hydrogen atom. The reason is that the non-relativistic boundstate theory based on perturbative QCD, by itself, was not successful for describing the heavy quarkonium states. The most serious problem has been the fact that perturbative QCD does not reproduce the shape of the static QCD potential $V_{\rm QCD}(r)$, which is considered to dictate a dominant part of the dynamics of these system, in the relevant region $0.5~{\rm GeV}^{-1} \lesssim r \lesssim 5~{\rm GeV}^{-1}$.

The theoretical method which has been widely used for analyses of the heavy quarkonium states is the phenomenological potential-model approach. In this method, one assumes some simple form for an effective (non-relativistic) Hamiltonian of the quarkonium system. A phenomenological potential, which is close to the above QCD potential conceptually, is introduced in the Hamiltonian. One parameterises the potential and determines the parameters such that various physical observables of the quarkonia are reproduced in this model. It turned out that phenomenological potentials determined in this way have more or less similar shapes in the region $0.5~{\rm GeV}^{-1} \lesssim r \lesssim 5~{\rm GeV}^{-1}$, which may be represented typically by a Coulomb-plus-linear potential. See e.g. Ref. [1] for a recent analysis based on potential models.

On the other hand, theoretical approaches, which have foundations on first principles, have been developed. Within the framework of Non-Relativistic QCD (NRQCD) or potential-NRQCD, the Lagrangian of a heavy quarkonium system is given in a series expansion of some small parameter (typically the quark velocity $v \sim \alpha_s$). The Wilson coefficients of the effective theory are determined by matching the theory to the full QCD theory either perturbatively or non-perturbatively. The QCD potential, as well as other (sub-leading) potentials which enter the effective theory, are determined from the results of lattice calculations or from model calculations; see [2] and references therein. The lattice results, being first principle calculations, turn out to be consistent with phenomenologically determined potentials, but at the present stage they are still not precise enough.

Computations of the QCD potential within perturbative QCD also made progress over time. The full two-loop corrections with massless quark loops [3], as well as non-zero mass effects in quark loops up to the same order [4–6], have been computed. The perturbative expansion at $r \gtrsim 0.2~{\rm GeV}^{-1}$ revealed to be very poorly convergent, and also its shape deviates qualitatively from an expected Coulomb-plus-linear form in the relevant range. The poor convergence is considered to reflect a non-trivial structure of the QCD vacuum. Also, within the context of perturbative QCD, this behaviour has been understood using the renormalon language [7].

Recently, there have been significant developments in the non-relativistic boundstate theory based on perturbative QCD. Thanks to the calculations of higher-order corrections [8–11] and the understanding of the leading renormalon cancellation [12, 13], it became possible to predict accurately the physical observables of the heavy quarkonium states (in particular, the bottomonium states) within perturbative QCD [5, 10, 14–19]. An essential feature is that the prediction for the QCD potential, after incorporating these developments, has become accurate, and that it has reproduced a realistic shape of the potential in the relevant range. Ref. [17] investigated this feature in particular. There, the following aspects have been shown:

(1) When the leading renormalon cancellation is incorporated, convergence property of the total energy of the bottomonium system $E_{\rm tot}(r) = 2m_{b,\rm pole} + V_{\rm QCD}(r)$ improves drastically.

(2) For simplicity, two hypothetical cases, $m_c \to 0$ and $m_c \to m_b$, have been examined; a reliable theoretical prediction for $E_{\rm tot}(r)$ is obtained at $r \lesssim 3\ {\rm GeV}^{-1}$, and the prediction agrees with typical phenomenological potentials in the range $0.5\ {\rm GeV}^{-1} \lesssim r \lesssim 3\ {\rm GeV}^{-1}$ within theoretical uncertainties.

(3) The qualitative behaviour of $E_{\rm tot}(r)$ in the above range can be understood as originating from an increase of the interquark force due to the running of the coupling constant.

In this paper we extend the analysis of [17]. First, we incorporate the realistic value of the charm mass in the calculation of $E_{\rm tot}(r)$. Since we are interested in the range of r not very different from the charm-mass scale $1/m_c$, we should properly take into account the dependence on m_c which enters through loop corrections. In this way we can compare predictions of perturbative QCD in the realistic case with phenomenological potentials. Secondly, we compute the total energies for quark-antiquark systems other than the $b\bar{b}$ system and compare them. In [17] the part of $E_{\rm tot}(r)$ independent of the external quark masses has been examined using the interquark force. Here we examine it in a different way. Our purpose is to compare the QCD potential (or the corresponding potential in the effective Hamiltonian of the quarkonium system), which has been studied in various approaches so far, with the prediction of perturbative QCD. We anticipate that, by combining our results with the conventional studies, we would be able to obtain a better understanding on the dynamics of the heavy quarkonia from first principles.

In Sec. 2 we compute the total energy of the $b\bar{b}$ system, incorporating non-zero charm mass effects: in Sec. 2.1 we set up our formulas; in Sec. 2.2 numerical analyses are given; in Sec. 2.3 we discuss uncertainties of our predictions. In Sec. 3 the total energies of other systems are examined. Conclusions are given in Sec. 4. Appendices collect some formulas.

2 Total Energy of the $b\bar{b}$ System

2.1 Definitions

In the $\overline{\rm MS}$ scheme, it is appropriate to compute the total energy of the $b\bar{b}$ system in the theory which contains 5 flavours. We are, however, interested in the total energy when the distance between b and $\bar{b}$ is much larger than their Compton wavelength, $r \gg 1/m_b$. Therefore, we will rewrite the total energy in terms of the 4-flavour coupling $\alpha_S^{(4)}(\mu)$ in order to realize decoupling of the b-quark to all orders.

When we neglect the charm quark mass, the total energy is given by

$$E^{b\bar{b}}_{{\rm tot},m_c=0}(r) = 2m_{b,\rm pole} + V_{{\rm QCD},4}(r). \tag{1}$$

The relation between the pole mass and the $\overline{\mathrm{MS}}$ mass has been computed up to 3 loops in a full theory, which contains n_h heavy flavours and n_l massless flavours [20]. (The same relation was obtained numerically in [21] in a certain approximation.) Setting $n_h = 1$ and rewriting the relation in terms of the coupling of the theory with $n_l = 4$ massless flavours only, we find[*]

$$m_{b,\mathrm{pole}} = \overline{m}_b \left\{ 1 + \frac{4}{3}\,\frac{\alpha_S^{(4)}(\overline{m}_b)}{\pi} + \left(\frac{\alpha_S^{(4)}(\overline{m}_b)}{\pi}\right)^2 d_1^{(4)} + \left(\frac{\alpha_S^{(4)}(\overline{m}_b)}{\pi}\right)^3 d_2^{(4)} \right\}, \tag{2}$$

where $\overline{m}_i \equiv m_i^{\overline{\mathrm{MS}}}(m_i^{\overline{\mathrm{MS}}})$ denotes the $\overline{\mathrm{MS}}$ mass renormalised at the $\overline{\mathrm{MS}}$-mass scale. The QCD potential of the theory with n_l massless flavours only[†] is given, up to $\mathcal{O}(\alpha_S^3)$, by

$$\begin{aligned} V_{\mathrm{QCD},n_l}(r) \;=\; & -\frac{4}{3}\frac{\alpha_S^{(n_l)}(\mu)}{r}\Bigg[1 + \left(\frac{\alpha_S^{(n_l)}(\mu)}{4\pi}\right)(2\beta_0^{(n_l)}\ell + a_1^{(n_l)}) \\ & + \left(\frac{\alpha_S^{(n_l)}(\mu)}{4\pi}\right)^2 \left\{ \left(\beta_0^{(n_l)}\right)^2 \left(4\ell^2 + \frac{\pi^2}{3}\right) + 2(\beta_1^{(n_l)} + 2\beta_0^{(n_l)} a_1^{(n_l)})\ell + a_2^{(n_l)} \right\} \Bigg], \end{aligned} \tag{3}$$

where $\ell = \log(\mu r) + \gamma_E$, and β_i denote the coefficients of the beta function

$$\beta_0^{(n_l)} = 11 - \frac{2}{3} n_l, \qquad \beta_1^{(n_l)} = 102 - \frac{38}{3} n_l. \tag{4}$$

The constants a_i and d_i are given in Appendix A.

When we include the effects of the non-zero charm-quark mass, the above formula is modified as follows:

$$E_{\mathrm{tot}}^{b\bar{b}}(r) = E_{\mathrm{tot},m_c=0}^{b\bar{b}}(r) + 2\,\delta m_{b,\mathrm{pole}} + \delta V_{\mathrm{QCD}}(r). \tag{5}$$

At $\mathcal{O}(\alpha_S^2)$ the non-zero charm mass correction to the pole mass, $\delta m_{b,\mathrm{pole}}$, reads [22]

$$\begin{aligned} \delta m_{b,\mathrm{pole}}^{[2]} \;=\; & \frac{\overline{m}_b}{3}\left(\frac{\alpha_S^{(4)}(\overline{m}_b)}{\pi}\right)^2 \Bigg[\log^2(\xi) + \frac{\pi^2}{6} - \left(\log(\xi) + \frac{3}{2}\right)\xi^2 \\ & + (1+\xi)(1+\xi^3)\left(\mathrm{Li}_2(-\xi) - \frac{1}{2}\log^2(\xi) + \log(\xi)\log(1+\xi) + \frac{\pi^2}{6}\right) \\ & + (1-\xi)(1-\xi^3)\left(\mathrm{Li}_2(\xi) - \frac{1}{2}\log^2(\xi) + \log(\xi)\log(1-\xi) - \frac{\pi^2}{3}\right)\Bigg], \end{aligned} \tag{6}$$

where $\xi = \overline{m}_c/\overline{m}_b$. Its leading term in the limit $m_c \to 0$ (linear approximation) is given by

$$\left.\delta m_{b,\mathrm{pole}}^{[2]}\right|_{m_c\to 0} = \frac{(\alpha_S^{(4)}(\overline{m}_b))^2}{6}\overline{m}_c. \tag{7}$$

---

[*] This relation coincides with Eq.(14) of [20], which is given numerically (indirectly through β_0 and β_1). Note that, in the other formulas of [20], the coupling of the full theory is used.

[†] Due to the decoupling theorem, the perturbative QCD potential of the theory which contains one heavy flavour (with mass m) and n_l massless flavours coincides with the potential in Eq. (3) up to $\mathcal{O}(\alpha_S^3)$ if we count $1/r = \mathcal{O}(\alpha_S m)$ and if we rewrite the coupling by the coupling of the theory with n_l massless flavours only.

At $\mathcal{O}(\alpha_S^3)$, the complete expression of $\delta m_{b,\rm pole}$ is not known; it has been computed only in the linear approximation [5]:

$$\begin{aligned}
\delta m^{[3]}_{b,\rm pole}\Big|_{m_c\to 0} &= \frac{(\alpha_S^{(4)}(\overline{m}_b))^3}{\pi}\overline{m}_c \left\{ \frac{2}{9} + \frac{\beta_0^{(4)}}{12}\left(-2\log(\xi) - 4\log 2 + \frac{14}{3}\right)\right. \\
&\qquad \left. -\frac{1}{9}\left(\frac{59}{15} + 2\log 2\right) + \frac{19}{9\pi}(f_1 f_2 + b_1 b_2)\right\}, \qquad (8)
\end{aligned}$$

where $f_2 = 0.470 \pm 0.005$, $b_2 = 1.120 \pm 0.010$, $f_1 = (\log A - \log b_2)/(\log f_2 - \log b_2)$, $b_1 = (\log A - \log f_2)/(\log b_2 - \log f_2)$ and $\log A = 161/228 + 13\zeta_3/19 - \log 2$. In [5] it has been argued that the use of the linear approximation in both $\delta m^{[2]}_{b,\rm pole}$ and $\delta m^{[3]}_{b,\rm pole}$ is a slightly better approximation of the full result than to use the exact $\delta m^{[2]}_{b,\rm pole}$ and the linear approximation of $\delta m^{[3]}_{b,\rm pole}$. It has been conjectured that the former approximation accounts for the full correction $\delta m^{[2]}_{b,\rm pole} + \delta m^{[3]}_{b,\rm pole}$ with about 10% accuracy, while the latter approximation accounts for the full result with about 20% accuracy. In [19], the theoretical predictions for the bottomonium energy levels turned out to be more stable when we used $(\delta m^{[2]}_{b,\rm pole}|_{m_c\to 0}) + (\delta m^{[3]}_{b,\rm pole}|_{m_c\to 0})$ as compared to $\delta m^{[2]}_{b,\rm pole} + (\delta m^{[3]}_{b,\rm pole}|_{m_c\to 0})$.

At $\mathcal{O}(\alpha_S^2)$ the non-zero charm mass correction to the QCD potential, $\delta V_{\rm QCD}$, is given in one-parameter integral form as

$$\delta V^{[2]}_{\rm QCD}(r) = -\frac{4}{3}\frac{\alpha_S^{(4)}(\mu)}{r}\left(\frac{\alpha_S^{(4)}(\mu)}{3\pi}\right)\left[\int_1^\infty dx\, f(x)\, e^{-2\overline{m}_c r x} + \left(\log(\overline{m}_c r) + \gamma_E + \frac{5}{6}\right)\right] \qquad (9)$$

with

$$f(x) = \frac{\sqrt{x^2-1}}{x^2}\left(1 + \frac{1}{2x^2}\right). \qquad (10)$$

At $\mathcal{O}(\alpha_S^3)$, the correction was computed first in momentum-space in [4]. The Fourier transform was performed‡ and $\delta V^{[3]}_{\rm QCD}(r)$ was obtained also in one-parameter integral form in [5,6]. Both of the latter references contain misprints, however; for completeness, we give a corrected formula for $\delta V^{[3]}_{\rm QCD}(r)$ in Appendix B.§

Since the renormalon cancellation at each order of the perturbative expansion is realized only when we use the same coupling constant in expanding $m_{b,\rm pole}$ and $V_{{\rm QCD},4}(r)$, we rewrite $\alpha_S(\overline{m}_b)$ in terms of $\alpha_S(\mu)$ using the renormalization-group evolution of the coupling constant:

$$\begin{aligned}
\alpha_S^{(n_l)}(\overline{m}_i) &= \alpha_S^{(n_l)}(\mu)\left\{1 + \frac{\alpha_S^{(n_l)}(\mu)}{\pi}\frac{\beta_0^{(n_l)}}{2}\log\left(\frac{\mu}{\overline{m}_i}\right)\right. \\
&\qquad \left. + \left(\frac{\alpha_S^{(n_l)}(\mu)}{\pi}\right)^2\left[\frac{\beta_0^{(n_l)\,2}}{4}\log^2\left(\frac{\mu}{\overline{m}_i}\right) + \frac{\beta_1^{(n_l)}}{8}\log\left(\frac{\mu}{\overline{m}_i}\right)\right]\right\}. \qquad (11)
\end{aligned}$$

---

‡ The coordinate-space potential was studied using different integral representations in [4].

§ The corrected formula has been acknowledged by the author of [5].

Furthermore, we also examine the total energy after re-expressing it in terms of the 3-flavour coupling and compare it with the 4-flavour coupling case. This is because we are interested in the total energy in the range 0.5 $\text{GeV}^{-1} \lesssim r \lesssim 5\ \text{GeV}^{-1}$, where the charm quark may decouple as well. We insert the relation [23]

$$\alpha_S^{(4)}(\mu) = \alpha_S^{(3)}(\mu) \Biggl\{ 1 + \frac{\alpha_S^{(3)}(\mu)}{3\pi} \log\left(\frac{\mu}{\overline{m}_c}\right) + \left(\frac{\alpha_S^{(3)}(\mu)}{\pi}\right)^2 \left[\frac{1}{9}\log^2\left(\frac{\mu}{\overline{m}_c}\right) + \frac{19}{12}\log\left(\frac{\mu}{\overline{m}_c}\right) - \frac{11}{72}\right] \Biggr\} \tag{12}$$

into the above $E_{\text{tot}}^{b\bar{b}}(r)$ and re-expand in $\alpha_S^{(3)}(\mu)$. Thus, we will examine the series expansion of $E_{\text{tot}}^{b\bar{b}}(r; \overline{m}_b, \overline{m}_c, \alpha_S^{(n_l)}(\mu))$ in $\alpha_S^{(n_l)}(\mu)$ up to $\mathcal{O}((\alpha_S^{(n_l)})^3)$ for $n_l = 3$ and 4.

The obtained total energy depends on the scale μ due to truncation of the series at a finite order. Following the prescriptions of [17], we will fix the scale μ in the two different ways described below:

1. We fix the scale $\mu = \mu_1(r)$ by demanding stability of $E_{\text{tot}}(r)$ against variation of the scale:

$$\mu \frac{d}{d\mu} E_{\text{tot}}(r; \overline{m}_i, \alpha_S(\mu)) \Big|_{\mu=\mu_1(r)} = 0. \tag{13}$$

2. We fix the scale $\mu = \mu_2(r)$ on the minimum of the absolute value of the last known term [$\mathcal{O}(\alpha_S^3)$ term] of $E_{\text{tot}}(r)$:

$$\mu \frac{d}{d\mu} \left[E_{\text{tot}}^{[3]}(r; \overline{m}_i, \alpha_S(\mu)) \right]^2 \Big|_{\mu=\mu_2(r)} = 0. \tag{14}$$

2.2 Numerical Analyses

In this subsection we take the input value for the coupling constant as $\alpha_S^{(5)}(M_Z) = 0.1181 \pm 0.0020$ [24]. We evolve the coupling by solving the 3-loop renormalization-group equation numerically and match it to the 4- and 3-flavour couplings successively through the matching condition [23].¶ For the bottom- and charm-quark masses, we use the values $\overline{m}_b = 4.190^{-20}_{+19}$ GeV [19] and $\overline{m}_c = 1.243$ GeV [16], respectively. (For simplicity we do not change the value of $\overline{m}_c$ as a function of $\alpha_S^{(5)}(M_Z)$. This is justified, since the dependence of $E_{\text{tot}}(r)$ on it is much smaller than other theoretical uncertainties; see Sec. 2.3.) We compute both $\delta m_{b,\text{pole}}^{[2]}$ and $\delta m_{b,\text{pole}}^{[3]}$ in the linear approximation in this subsection.

First we examine the scale dependences of E_{tot} and $\left[E_{\text{tot}}^{[3]}(r; \overline{m}_i, \alpha_S(\mu))\right]^2$ in Eqs. (13) and (14). In the first scale-fixing prescription, the minimal sensitivity scale $\mu_1(r)$ exists only in the range $r \lesssim 3\ \text{GeV}^{-1}$. In the second prescription, $\mu = \mu_2(r)$, the minimum value of $|E_{\text{tot}}^{[3]}(r)|$ is

---

¶ The matching scales are taken as $\overline{m}_b$ and $\overline{m}_c$, respectively.

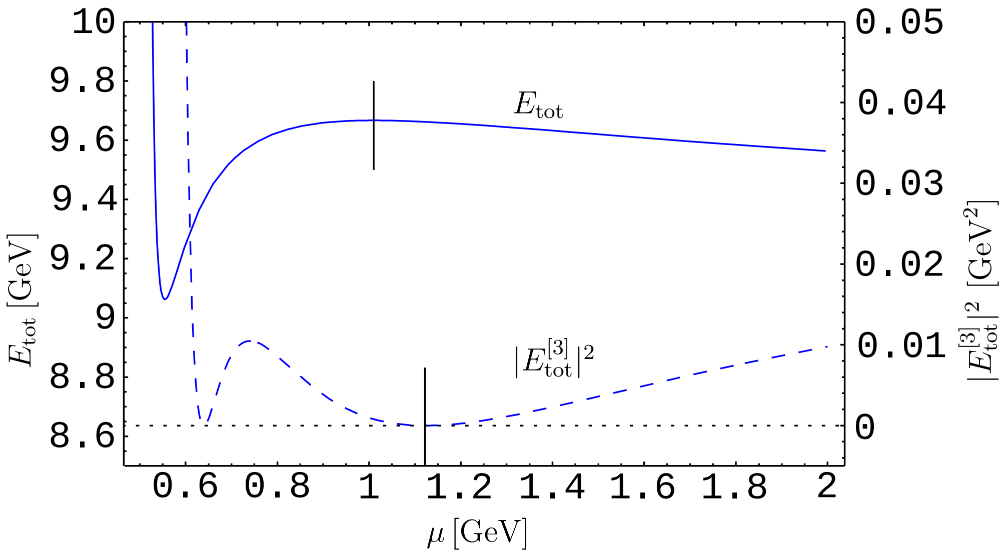

Figure 1: Determination of the scale: Total energy and α_s^3-term of the total energy, the scales determined with the respective prescription are marked with a short vertical line. (We do not take the scales which are located close to the infrared singularity of $\alpha_S^{(3)}(\mu)$.) The distance r is fixed to 2 GeV^{-1}; $\alpha_S^{(5)}(M_Z) = 0.1181$.

zero in the range $r \lesssim 3$ GeV^{-1}, whereas $|E_{\rm tot}^{[3]}(r)| > 0$ in the range $r \gtrsim 3$ GeV^{-1}. These features indicate an instability of the perturbative prediction for $E_{\rm tot}(r)$ at $r \gtrsim 3$ GeV^{-1}. Qualitative features of the scale dependences are similar for the expansions in the 3-flavour and the 4-flavour couplings. (They are also similar to the results of the analysis for $m_c \to 0$ or $m_c \to m_b$ [17].) The range where the prediction is stable extends to slightly longer distances for the 3-flavour case, in accord with our naive expectation. The scale-dependence is demonstrated in Fig. 1 for $r = 2$ GeV^{-1} and for the expansion in the 3-flavour coupling. We compare the total energy determined in the four different prescriptions (scale-fixing prescriptions 1 and 2, and expansions in $\alpha_S^{(3)}$ and $\alpha_S^{(4)}$) in Fig. 2. All four curves agree well in the range where both scale-fixing prescriptions exist. The numerical values of the total energy and the scale are listed in Table 1. We observe a strong cancellation of the leading renormalon between the pole mass and the QCD potential: the expansion of $E_{\rm tot}(r)$ is much more convergent than the expansions of the individual terms. This is demonstrated in Table 2.

Since the new aspect of our analysis is the inclusion of the charm-mass effects, we compare our result with those of the analysis done in the two hypothetical cases $m_c \to 0$ and $m_c \to m_b$. This is shown in Fig. 3. Our curve lies between those of the two hypothetical cases, which is consistent with our expectation.

Now we compare the total energy $E_{\rm tot}(r)$, as obtained above, with typical phenomenological potentials in the literature:

- A Coulomb-plus-linear potential (Cornell potential) [25]:

$$V(r) = -\frac{\kappa}{r} + \frac{r}{a^2} \qquad (15)$$

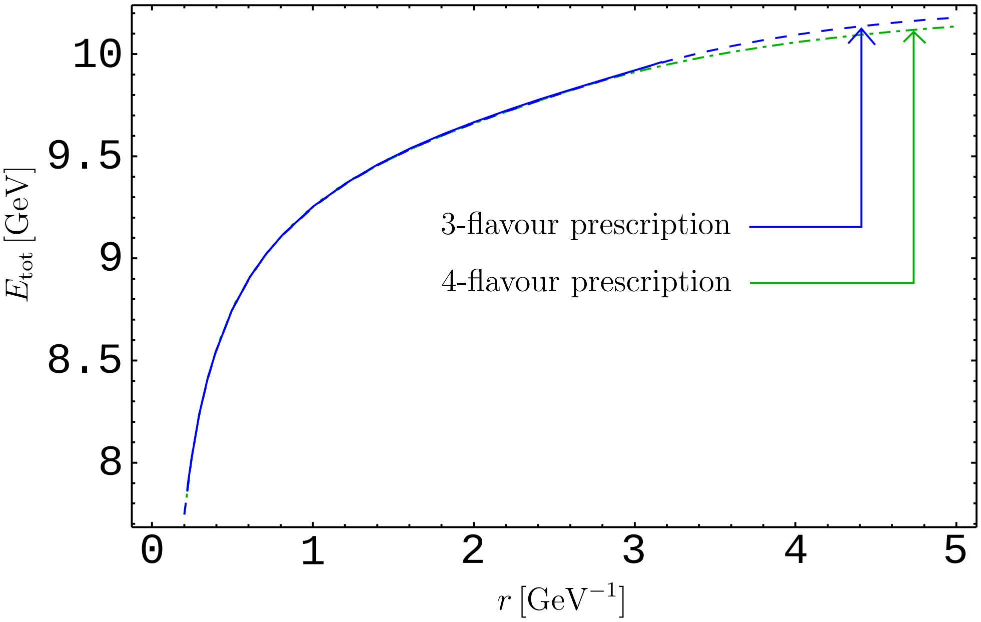

Figure 2: Total energy for 3-flavour ($\mu = \mu_1$: solid, $\mu = \mu_2$: dashed) and 4-flavour ($\mu = \mu_1$: dotted, $\mu = \mu_2$: dash-dotted) case. For the 3- (4-) flavour case prescription 1 breaks down at $r \approx 3.2\,(2.75)$ GeV^{-1}. Where both scale prescriptions exist, the curves coincide. $\alpha_S^{(5)}(M_Z) = 0.1181$.

r [GeV^{-1}]	$E_{\mathrm{tot}}(r)$ [GeV]	$\mu_2(r)$ [GeV]
0.5	8.75	1.99
1.0	9.25	1.52
1.5	9.49	1.28
2.0	9.66	1.12
2.5	9.79	0.98
3.0	9.92	0.79

Table 1: Comparison of the total energies and scales for the $b\bar{b}$ system (3–flavour prescription, $\mu = \mu_2$, $\alpha_S^{(5)}(M_Z) = 0.1181$).

n	$m_{b,\text{pole}}^{[n]}$	$\delta m_{b,\text{pole}}^{[n]}$	$V_{\text{QCD}}^{[n]}$	$\delta V_{\text{QCD}}^{[n]}$	$E_{\text{tot}}^{[n]}$
0	4.190	0	0	0	8.380
1	0.657	0	-0.493	0	0.822
2	0.175	0.028	-0.298	-0.032	0.076
3	0.182	0.044	-0.391	-0.084	-0.024

Table 2: Renormalon cancellation in the $b\bar{b}$ system ($r = 1$ GeV^{-1}, $\mu = \mu_1$, 3–flavour prescription, $\alpha_S^{(5)}(M_Z) = 0.1181$): The α_S–expansion of E_{tot} has much better convergence properties than the expansions of the individual terms. $X^{[n]}$ represents the order $(\alpha_S^{(3)}(\mu))^n$ term of X. $m_{b,\text{pole}}$ and V_{QCD} do not contain the m_c–effects, these are given as $\delta m_{b,\text{pole}}$ and δV_{QCD}. The units are GeV.

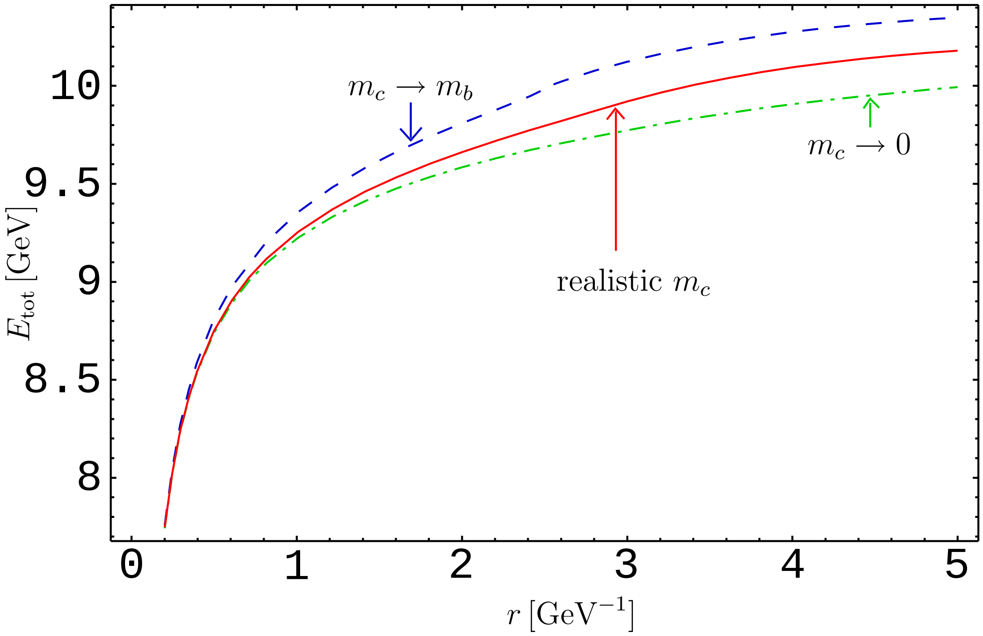

Figure 3: Charm mass effects: Comparison of the QCD potential for realistic m_c with the two limiting cases $m_c \rightarrow 0$ (1 heavy flavour, 4 light flavours) and $m_c \rightarrow m_b$ (2 heavy flavours, 3 light flavours) for $\alpha_S^{(5)}(M_Z) = 0.1181$.

with $\kappa = 0.52$ and $a = 2.34$ GeV^{-1}.

- A power-law potential [26]:

$$V(r) = -8.064 \text{ GeV} + (6.898 \text{ GeV})(r \times 1 \text{ GeV})^{0.1}. \tag{16}$$

- A logarithmic potential [27]:

$$V(r) = -0.6635 \text{ GeV} + (0.733 \text{ GeV}) \log(r \times 1 \text{ GeV}). \tag{17}$$

In Fig. 4 we compare these potentials with the perturbative computation of $E_{\rm tot}(r)$ for the input values $\alpha_S^{(5)}(M_Z) = 0.1181 \pm 0.0020$. An arbitrary constant is added to each potential, as well as to $E_{\rm tot}(r)$, such that it coincides with $E_{\rm tot}(r)$ for $\alpha_S^{(5)}(M_Z) = 0.1181$ at $r = 1$ GeV^{-1}.[‖] This is because the constant part (r-independent part) of each phenomenological potential is not determined well. As can be seen, $E_{\rm tot}(r)$ and the phenomenological potentials agree inside the errors estimated from the next-to-leading renormalons $\pm\frac{1}{2}\Lambda_{\rm QCD}(\Lambda_{\rm QCD}\cdot r)^2$ (taking $\Lambda_{\rm QCD} = 300$ MeV, indicated by error-bars), and the agreement is better for a larger value of the input parameter $\alpha_S^{(5)}(M_Z)$.

In order to quantify the differences between the phenomenological potentials and the QCD potential for different values of $\alpha_S(M_Z)$, we define a weighted difference between $E_{\rm tot}(r)$ and a potential $V(r)$ as

$$\Delta_n[E_{\rm tot}(r) - V(r)] = \min_c \int_{r_0}^{r_1} dr\, r^n \, |E_{\rm tot}(r) - V(r) - c|^2. \tag{18}$$

The minimum value of the integral is taken as we vary an arbitrary constant added to the potential. We examined the difference Δ_n between $E_{\rm tot}(r)$ and each of the phenomenological potentials, as well as Δ_n between $E_{\rm tot}(r)$ and the average of the three phenomenological potentials, for $n = -1$, 0 and +1. We found similar qualitative features: Δ_n becomes small for a larger value of $\alpha_S^{(5)}(M_Z)$, inside the present error, around 0.1191–0.1201. We demonstrate this in Fig. 5: $\Delta_{n=0}$ with $r_0 = 1$ GeV^{-1} and $r_1 = 4$ GeV^{-1} is shown for each of the potentials and for the averaged potential, varying the value of $\alpha_S(M_Z)$.

2.3 Error Estimates

There are several uncertainties in our theoretical prediction for the total energy $E_{\rm tot}^{b\bar{b}}(r)$.

(i) *Errors of the input parameters $\alpha_S^{(5)}(M_Z)$, $\overline{m}_b$ and $\overline{m}_c$:*
In Fig. 4 the dependence of $E_{\rm tot}(r)$ on $\alpha_S(M_Z)$ is shown. As $\alpha_S(M_Z)$ increases, $E_{\rm tot}(r)$ becomes steeper due to an increase of the interquark force [17]. Variation of $E_{\rm tot}$ at

---

[‖] The choice of r, where the potentials are made to coincide, is to some extent arbitrary. (Our choice $r = 1$ GeV^{-1} corresponds approximately to the root-mean-square radius of the $\Upsilon(1S)$ state, the heaviest state used to determine the phenomenological potentials.) The important point here is that we can indeed choose an additive constant such that $E_{\rm tot}(r)$ can be made to agree with the phenomenological potentials inside the estimated errors.

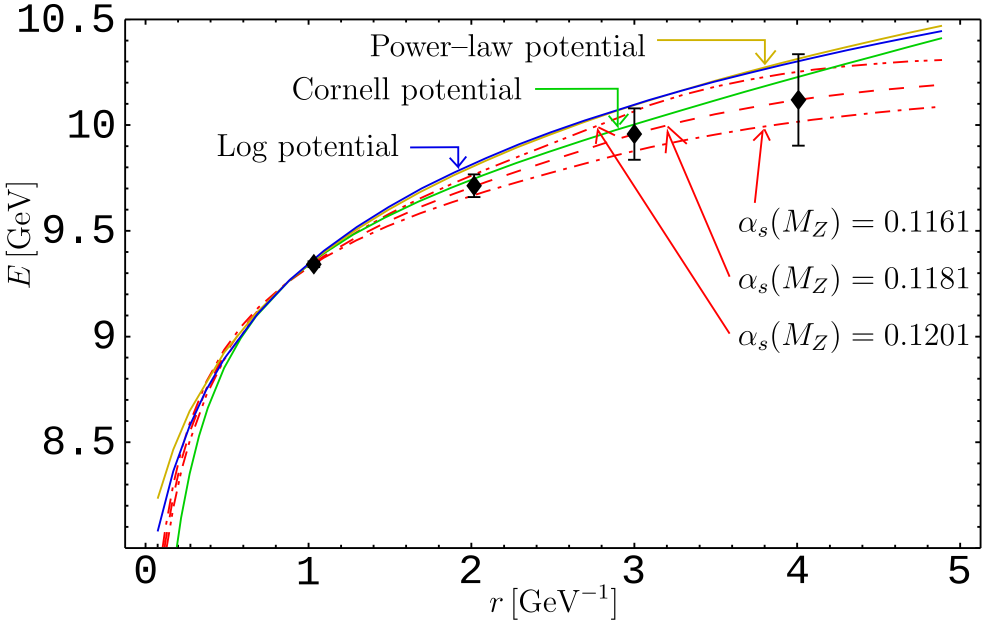

Figure 4: Comparison of the QCD potential to various models. The QCD potential is given for three values of $\alpha_S^{(5)}(M_Z)$, constants are added to make all curves coincide with the QCD potential ($\alpha_S^{(5)}(M_Z) = 0.1181$) at $r = 1$ GeV^{-1}.

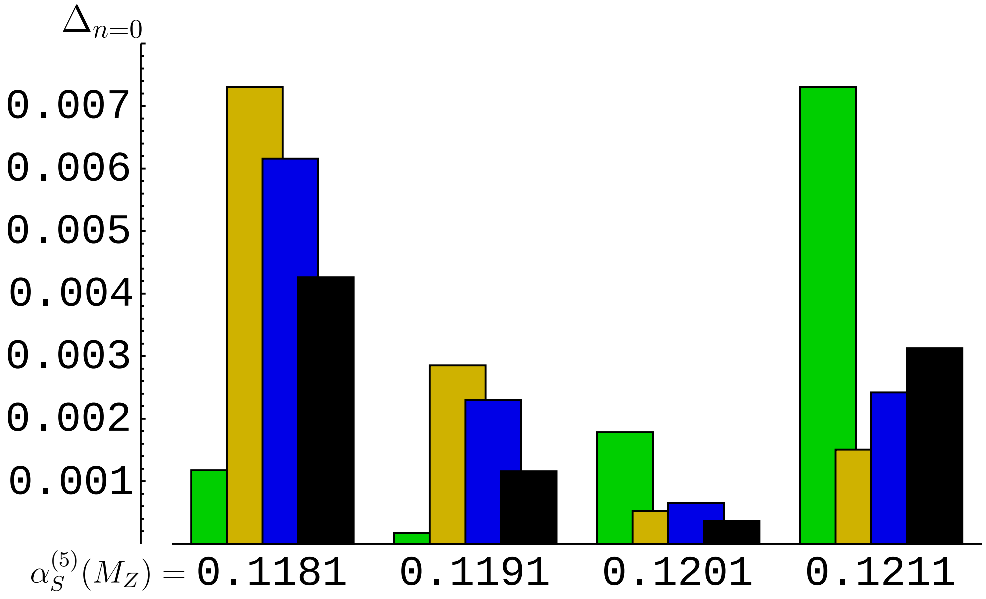

Figure 5: A comparison of the QCD potential for different $\alpha_S^{(5)}(M_Z)$ to various models. The height of the bars indicate the minimised difference $\Delta_{n=0}$ between the QCD potential and the model when varying the constant term. The four bars in each group correspond to (from left to right): Cornell potential, power–law potential, log potential and the average of the former three.

$r = 3\ \mathrm{GeV}^{-1}$ is about ±90 MeV with respect to its value at $r = 1\ \mathrm{GeV}^{-1}$, corresponding to a variation $\alpha_S^{(5)}(M_Z) = 0.1181 \pm 0.0020$. The present uncertainties of the b-quark and c-quark $\overline{\mathrm{MS}}$ masses are about ±30 MeV [19] and ±100 MeV [16,28], respectively, and also their central values are correlated with the value of $\alpha_S(M_Z)$. The dependence of $E_{\mathrm{tot}}(r)$ on $\overline{m}_b$ for small variations of $\overline{m}_b$ is practically a shift of $E_{\mathrm{tot}}(r)$ by $2\Delta\overline{m}_b$ (independent of r). We have confirmed this feature up to a larger variation of $\Delta\overline{m}_b = \pm 60$ MeV, corresponding to more conservative error estimates in the literature. The dependence of $E_{\mathrm{tot}}(r)$ on $\overline{m}_c$ is weak and negligible ($|\Delta E_{\mathrm{tot}}(r)| \lesssim 10$ MeV for $\Delta\overline{m}_c = \pm 100$ MeV), since the charm mass effects are $\mathcal{O}(\alpha_S^2)$ and beyond. Hence, of these only the dependence on $\alpha_S(M_Z)$ matters in the comparison of $E_{\mathrm{tot}}(r)$ and the phenomenological potentials.

(ii) *Unknown higher-order corrections*:
We may estimate the higher-order uncertainties from the size of the next-to-leading renormalon [7,17]. We show its typical size $\pm\frac{1}{2}\Lambda_{\mathrm{QCD}}(\Lambda_{\mathrm{QCD}} \cdot r)^2$ by error-bars in Fig. 4 taking $\Lambda_{\mathrm{QCD}} = 300$ MeV. We have also checked these estimates by computing the $\mathcal{O}(\alpha_S^4)$ correction to $E_{\mathrm{tot}}(r)$ in the large-β_0 approximation. The corrections from the $\mathcal{O}(\alpha_S^4)$-term are 7, 47, 68 MeV at $r = 1, 2, 3\ \mathrm{GeV}^{-1}$, respectively.

(iii) *Approximations in $\delta m_{b,\mathrm{pole}}$*:
In Sec. 2.2 the charm mass corrections to the pole mass, $\delta m_{b,\mathrm{pole}}^{[2]}$ and $\delta m_{b,\mathrm{pole}}^{[3]}$, have been computed in the linear approximation. We estimate uncertainties induced by this approximation by using the full correction Eq. (6) for $\delta m_{b,\mathrm{pole}}^{[2]}$ instead, while keeping $\delta m_{b,\mathrm{pole}}^{[3]}$ in the linear approximation. We find that $E_{\mathrm{tot}}(r)$ varies by -7, -10, -17 MeV at $r = 1, 2, 3\ \mathrm{GeV}^{-1}$, respectively.

(iv) *Non-perturbative effects*:
Up to now there exists no reliable way to estimate entire non-perturbative effects on the QCD potential accurately [2]. Moreover, in principle, the size of non-perturbative effects will depend on the specific perturbative scheme used in the computation of the QCD potential or the total energy. Here, we do not attempt to compute non-perturbative effects separately, but rather consider the differences between our predictions (with respective perturbative errors) and the phenomenological potentials as orders of magnitude estimates of non-perturbative effects in our computational scheme. From our present results, we may consider that non-perturbative effects would be absorbed into perturbative uncertainties of our predictions. This is consistent with the observation of [19].

Besides, when we compare our theoretical predictions with phenomenological potentials, we should take into account the following uncertainty:

(v) *Phenomenological Potentials vs. $E_{\mathrm{tot}}^{b\bar{b}}(r)$*:
Our ultimate goal would be to compare the exact QCD potential with the perturbative prediction (after subtracting renormalons). The phenomenological potentials are not direct physical observables but are determined under certain model assumptions. Since separation of the QCD potential from the rest of the interactions (e.g. $1/r^2$ potential,

relativistic corrections) is not absolutely clear in the phenomenological approaches, there may be substantial corrections between the phenomenological potentials and the QCD potential or the total energy $E_{\rm tot}^{b\bar{b}}(r)$. The relation can only be clarified by detailed comparisons of the predictions of perturbative QCD with the experimental data for various physical observables of the bottomonium states, such as the energy spectrum, decay rates, level-transition rates, etc. (Studies on the energy levels have been initiated in [16, 19]). These detailed comparisons, however, are beyond the scope of the present paper.

3 Other Systems

Let us also examine the total energies of other quark-antiquark systems. Theoretically we may expect that a limit of the potential energy exists when we send the masses of quark and antiquark to infinity. Empirically both the bottomonium and charmonium spectra can be reproduced well with the same phenomenological potential. Thus, it would be interesting to examine whether the total energies for different systems coincide up to an additive constant.

For the $b\bar{c}$ system, we consider

$$E_{\rm tot}^{b\bar{c}}(r) = m_{b,\rm pole} + \delta m_{b,\rm pole} + m_{c,\rm pole} + V_{\rm QCD,4}(r) + \delta V_{\rm QCD}(r), \tag{19}$$

where

$$m_{c,\rm pole} = \overline{m}_c \left\{ 1 + \frac{4}{3}\,\frac{\alpha_S^{(3)}(\overline{m}_c)}{\pi} + \left(\frac{\alpha_S^{(3)}(\overline{m}_c)}{\pi}\right)^2 d_1^{(3)} + \left(\frac{\alpha_S^{(3)}(\overline{m}_c)}{\pi}\right)^3 d_2^{(3)} \right\}. \tag{20}$$

We examine the expansions of $E_{\rm tot}^{b\bar{c}}(r)$ both in the 4-flavour and 3-flavour couplings, and in the two scale-fixing prescriptions Eqs. (13) and (14). We find that, at distances $0.5~{\rm GeV}^{-1} \lesssim r \lesssim 1.8~{\rm GeV}^{-1}$, $\mu_1(r)$ exists in the first prescription and the minimim value of $|E_{\rm tot}^{[3]}|$ is zero in the second prescription, indicating that stable theoretical predictions for the total energy are obtained in this region. A comparison in Fig. 6 shows that the predictions for the total energies of the $b\bar{c}$ system and $b\bar{b}$ system agree within the uncertainties of the predictions. We also note that, even at $r \gtrsim 1.8~{\rm GeV}^{-1}$, where only the second scale-fixing prescription exists, the curves for the $b\bar{c}$ system in the 4-flavour and 3-flavour couplings agree with each other and they are also consistent with that of the $b\bar{b}$ system. See also Tables 3 and 4 for numerical values.

Furthermore we examined the total energy of the $c\bar{c}$ system,

$$E_{\rm tot}^{c\bar{c}}(r) = 2m_{c,\rm pole} + V_{\rm QCD,3}(r), \tag{21}$$

in a similar way. We, however, obtained stable predictions only in the very narrow vicinity of $r \simeq 1~{\rm GeV}^{-1}$ and consequently we could not compare the shape of $E_{\rm tot}(r)$ with that of the $b\bar{b}$ or $b\bar{c}$ system. We believe that this is caused by the typical scales for the $c\bar{c}$ system being too low to give reliable perturbative expansions. (We may compare this feature with that of the perturbative calculation of the energy levels of charmonium [16]: only the $1S$ levels can be computed reliably.)

r [GeV^{-1}]	$E_{\rm tot}(r)$ [GeV]	$\mu_2(r)$ [GeV]
0.5	5.35	4.08
1.0	5.85	1.31
1.5	6.12	0.97
2.0	6.34	0.76
2.5	6.48	0.83
3.0	6.55	0.93

Table 3: Comparison of the total energies and scales for the $b\bar{c}$ system (3–flavour prescription, μ_2). The predictions are stable in the range 0.5 GeV^{-1} $\lesssim r \lesssim$ 1.8 GeV^{-1}.

n	$m_{b,\rm pole}^{[n]}$	$\delta m_{b,\rm pole}^{[n]}$	$m_{c,\rm pole}^{[n]}$	$V_{\rm QCD}^{[n]}$	$\delta V_{\rm QCD}^{[n]}$	$E_{\rm tot}^{[n]}$
0	4.190	0	1.243	0	0	5.433
1	0.730	0	0.217	−0.547	0	0.399
2	0.153	0.035	0.211	−0.321	−0.039	0.038
3	0.203	0.054	0.304	−0.466	−0.109	−0.014

Table 4: Renormalon cancellation in the $b\bar{c}$ system ($r = 1$ GeV^{-1}, $\mu = \mu_1$, 3–flavour prescription). Notations are same as in Table 2.

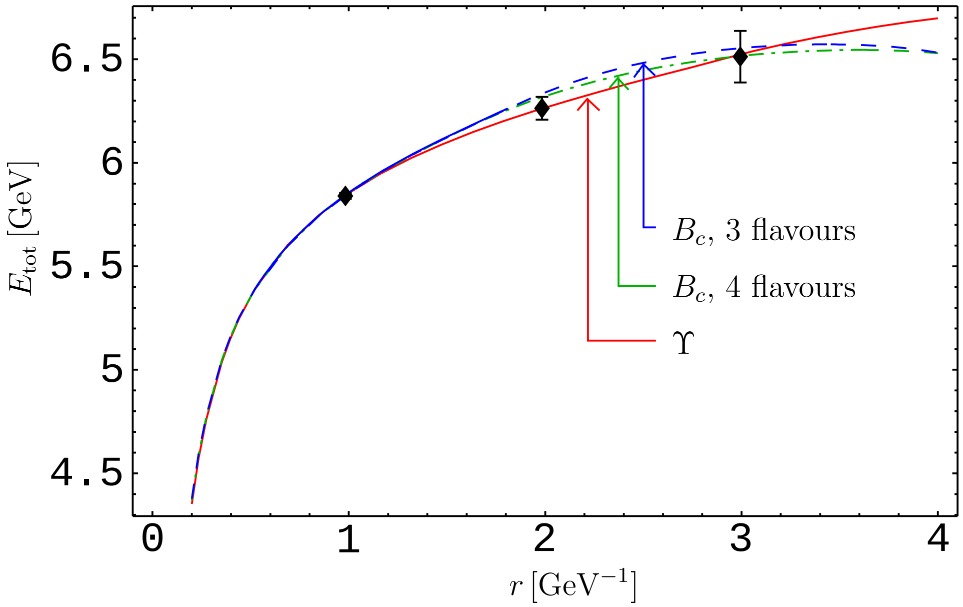

Figure 6: Total energy of the B_c–system for 3-flavour ($\mu = \mu_1$: solid, $\mu = \mu_2$: dashed) and 4-flavour ($\mu = \mu_1$: dotted, $\mu = \mu_2$: dash-dotted) prescription. For comparison the energy of the Υ–system (3 flavours) is shown (shifted so that it coincides with the B_c energy at $r = 1$ GeV^{-1}). For all curves $\alpha_S^{(5)}(M_Z) = 0.1181$. Error-bars indicate $\pm\frac{1}{2}\Lambda_{\rm QCD}(\Lambda_{\rm QCD}\cdot r)^2$ with $\Lambda_{\rm QCD} = 300$ MeV.

Conversely we examined the total energy of the $b\bar{b}$ system as we increase the bottom quark mass artificially. When we do this, we find that the region of r, where we can make a stable prediction of $E_{\rm tot}(r)$, shifts to shorter distances. In other words, we can still make a stable prediction of the shape of the potential from the distance $r \simeq 1/\overline{m}_b$ up to the region which is relevant to the formation of the (hypothetically heavy) bottomonium states. This is reasonable, since a heavier quarkonium has a smaller radius, and the prediction should be stable for this smaller radius. On the other hand, we do not always have stable predictions for $E_{\rm tot}(r)$ in the region of our interest, $0.5~{\rm GeV}^{-1} \lesssim r \lesssim 5~{\rm GeV}^{-1}$. We may understand this property as a manifestation of a multi-scale problem. The pole mass contains powers of $\log(\mu/\overline{m}_b)$, while the QCD potential contains powers of $\log(\mu r)$. When $\overline{m}_b$ and r^{-1} are very different, it generally becomes more difficult to cancel two different types of logarithms, so it becomes difficult to find a scale μ which stabilizes the theoretical prediction. For a (hypothetical) value of $\overline{m}_b$ below about 23 GeV, we still have an overlap between the region of stable predictions for the total energy and the above region of our interest. Where both scale-fixing prescriptions exist, the predictions coincide. (The distance r where the minimum of $|E_{\rm tot}^{[3]}|$ deviates from zero in the second prescription is close to the distance beyond which the first scale $\mu_1(r)$ does not exist.) In the region where both prescriptions exist, the predictions agree with $E_{\rm tot}^{b\bar{b}}(r)$ computed with the realistic b-quark mass, up to an additive constant.* At larger r the larger mass produces a smaller total energy. This tendency is expected from the higher-order analysis in the large-β_0 approximation [17]. Also this agrees qualitatively with our results for the $b\bar{c}$ against $b\bar{b}$ system: from the point where the curves split, $E_{\rm tot}^{b\bar{c}}$ is larger than $E_{\rm tot}^{b\bar{b}}$, although the curves later cross (Fig. 6). These features are demonstrated in Fig. 7, where the total energy for $\overline{m}_b = 15$ GeV is shown and compared with the one with the realistic b-quark mass.

4 Conclusions

We have analysed the total energy of the $b\bar{b}$ system incorporating the non-zero charm-quark mass effects. We observed an improvement of convergence of the perturbative expansion, once we perform the cancellation of the leading renormalons; we obtained stable theoretical predictions for the total energy $E_{\rm tot}^{b\bar{b}}(r)$ at $r \lesssim 3~{\rm GeV}^{-1}$. These features are qualitatively the same as those observed in [17]. We compared the total energy with typical phenomenological potentials. They agree in the range $0.5~{\rm GeV}^{-1} \lesssim r \lesssim 3~{\rm GeV}^{-1}$ within the estimated theoretical uncertainties. The agreement becomes very good when the value of the input parameter $\alpha_S^{(5)}(M_Z)$ is large (inside the error bands), 0.1191–0.1201. From these results, we may conclude that, in analysing the nature of the bottomonium states, using the perturbative prediction for $E_{\rm tot}^{b\bar{b}}(r)$ is, at least, as good as using phenomenological potentials. We may compare our result with the comprehensive analysis of the bottomonium spectrum which includes full corrections up to $\mathcal{O}(1/c^2)$ [19]. There, a smaller value around 0.1161 for $\alpha_S^{(5)}(M_Z)$ was favored. Therefore, we see that the interactions other than $E_{\rm tot}(r)$ play non-negligible roles for the predictions of the

---

* Of course, the agreement is better at shorter distances, where the perturbative predictions tend to be more reliable. At $r \lesssim 1.5~{\rm GeV}^{-1}$ the expansion in the 4-flavour coupling tends to be more stable than the expansion in the 3-flavour coupling.

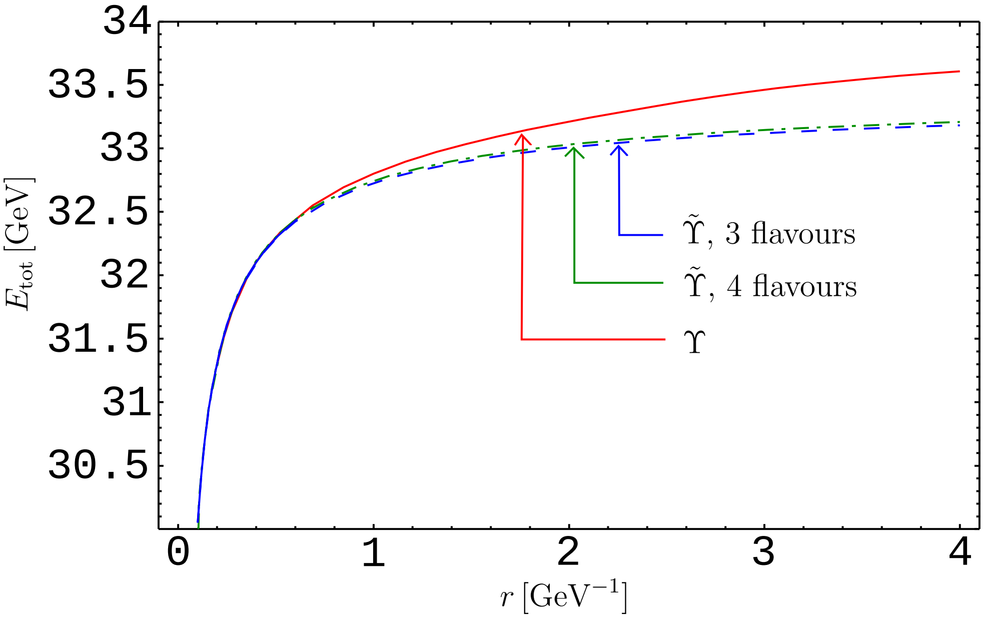

Figure 7: Total energy of the bound state $\tilde\Upsilon$ of a hypothetical heavy b–quark with a mass of 15 GeV in 3-flavour ($\mu = \mu_1$ [breaks down at $r \approx 0.6\,\mathrm{GeV}^{-1}$]: solid, $\mu = \mu_2$: dashed) and four flavour ($\mu = \mu_1$ [breaks down at $r \approx 0.8\,\mathrm{GeV}^{-1}$]: dotted, $\mu = \mu_2$: dash-dotted) prescription. Where both scale prescriptions exist, the curves coincide. For comparison the energy for the Υ–system (3 flavours) is shown (shifted so that it coincides with the $\tilde\Upsilon$ energy at $r = 0.5\,\mathrm{GeV}^{-1}$. For all curves $\alpha_S^{(5)}(M_Z) = 0.1181$.

bottomonium energy levels, with respect to the present theoretical accuracy of perturbative QCD.

We also examined the perturbative predictions for $E_{\rm tot}(r)$ of other systems. For the $b\bar{c}$ system, stable predictions are obtained (at least) in the range $r \lesssim 1.8$ GeV^{-1}. In this range, the total energy agrees with that of the $b\bar{b}$ system inside theoretical uncertainties. For the $c\bar{c}$ system, we could barely obtain stable theoretical predictions for the shape of $E_{\rm tot}(r)$, since the relevant scales are very low. We also found that, for a heavier (hypothetical) quarkonium system, the range where $E_{\rm tot}(r)$ can be predicted reliably, shifts to shorter distances. At any event, whenever we may obtain stable theoretical predictions for $E_{\rm tot}(r)$ at $r \gtrsim 0.5$ GeV^{-1}, the predictions agree with the phenomenological potentials within present theoretical uncertainties.

Appendix

A: Parameters

The constants used in Eqs. (2) and (3) are given by [3]

$$a_1^{(n_l)} = \frac{31}{3} - \frac{10}{9} n_l, \tag{22}$$

$$a_2^{(n_l)} = \frac{4343}{18} + 36\,\pi^2 + 66\,\zeta_3 - \frac{9\,\pi^4}{4} - n_l \left(\frac{1229}{27} + \frac{52\,\zeta_3}{3} \right) + \frac{100}{81}\, n_l^2, \tag{23}$$

and

$$\begin{aligned} d_1^{(n_l)} &= \frac{307}{32} + \frac{\pi^2}{3} + \frac{\pi^2\, \log 2}{9} - \frac{\zeta_3}{6} + n_l \left(-\frac{71}{144} - \frac{\pi^2}{18} \right) \\ &\simeq 13.4434 - 1.04137\, n_l, \end{aligned} \tag{24}$$

$$\begin{aligned} d_2^{(n_l)} &= \frac{8462917}{93312} + \frac{652841\,\pi^2}{38880} - \frac{695\,\pi^4}{7776} - \frac{575\,\pi^2\, \log 2}{162} \\ &\quad - \frac{22\,\pi^2 \log^2 2}{81} - \frac{55 \log^4 2}{162} - \frac{220\, {\rm Li}_4(\frac{1}{2})}{27} + \frac{58\,\zeta_3}{27} - \frac{1439\,\pi^2\,\zeta_3}{432} + \frac{1975\,\zeta_5}{216} \\ &\quad + n_l \left(-\frac{231847}{23328} - \frac{991\,\pi^2}{648} + \frac{61\,\pi^4}{1944} - \frac{11\,\pi^2\, \log 2}{81} + \frac{2\,\pi^2 \log^2 2}{81} + \frac{\log^4 2}{81} \right. \\ &\quad \left. + \frac{8\, {\rm Li}_4(\frac{1}{2})}{27} - \frac{241\,\zeta_3}{72} \right) + n_l^2 \left(\frac{2353}{23328} + \frac{13\,\pi^2}{324} + \frac{7\,\zeta_3}{54} \right) \\ &\simeq 190.391 - 26.6551\, n_l + 0.652691\, n_l^2. \end{aligned} \tag{25}$$

B: $\boldsymbol{\delta V^{[3]}_{\mathrm{QCD}}(r)}$

After correcting misprints in [5,6], the charm-mass correction to the QCD potential at $\mathcal{O}(\alpha_S^3)$ reads[†]

$$
\begin{aligned}
\delta V^{[3]}_{\mathrm{QCD}}(r) \;=\;& -\frac{4}{3}\,\frac{\alpha_S^{(4)}(\mu)}{r}\Big(\frac{\alpha_S^{(4)}(\mu)}{3\pi}\Big)^2\Bigg[\\
& \Bigg\{-\frac{3}{2}\int_1^\infty dx\, f(x)\, e^{-2\overline{m}_c r x}\Big(\beta_0^{(4)}\Big(\log\frac{4\overline{m}_c^2 x^2}{\mu^2} - \mathrm{Ei}(2\overline{m}_c r x) - e^{4\overline{m}_c r x}\mathrm{Ei}(-2\overline{m}_c r x)\Big) - a_1^{(4)}\Big)\\
& +3\,\Big(\log(\overline{m}_c r) + \gamma_E + \frac{5}{6}\Big)\Big(\beta_0^{(4)}\ell + \frac{a_1^{(4)}}{2}\Big) + \beta_0^{(4)}\,\frac{\pi^2}{4}\Bigg\}\\
-\;& \Bigg\{\int_1^\infty dx\, f(x)\, e^{-2\overline{m}_c r x}\Big(\frac{1}{x^2} + x\, f(x)\,\log\frac{x-\sqrt{x^2-1}}{x+\sqrt{x^2-1}}\Big)\\
& +\int_1^\infty dx\, f(x)\, e^{-2\overline{m}_c r x}\Big(\log 4x^2 - \mathrm{Ei}(2\overline{m}_c r x) - e^{4\overline{m}_c r x}\mathrm{Ei}(-2\overline{m}_c r x)\Big)\\
& -\Big(\log(\overline{m}_c r) + \gamma_E + \frac{5}{6}\Big)^2 - \frac{\pi^2}{12}\Bigg\}\\
+\;& \Bigg\{\frac{57}{4}\Big(f_1\,\Gamma(0, 2f_2\overline{m}_c r) + b_1\,\Gamma(0, 2b_2\overline{m}_c r) + \log(\overline{m}_c r) + \gamma_E + \frac{161}{228} + \frac{13}{19}\zeta_3\Big)\Bigg\}\\
+\;& \Bigg\{\int_1^\infty dx\, f(x)\, e^{-2\overline{m}_c r x}\Big(-8\overline{m}_c r x\Big) + 4\Bigg\}\Bigg]. \qquad (26)
\end{aligned}
$$

Acknowledgements

Y.S. is grateful to Y. Kiyo for fruitful discussion. S.R. was supported by the Japan Society for the Promotion of Science (JSPS).

References

[1] E. Eichten and C. Quigg, Phys. Rev. **D49**, 5845 (1994).

[2] G. Bali, Phys. Rep. **343**, 1 (2001).

[3] M. Peter, Phys. Rev. Lett. **78**, 602 (1997); Nucl. Phys. **B501** 471 (1997); Y. Schröder, Phys. Lett. **B447**, 321 (1999).

[4] M. Melles, Phys. Rev. **D62**, 074019 (2000).

[5] A. Hoang, hep-ph/0008102.

[6] M. Melles, Nucl. Phys. Proc. Suppl. **96**, 472 (2001).

[†] The last line stems from our use of $\overline{m}_c$ instead of the pole mass, and it is not due to the misprint.

[7] U. Aglietti and Z. Ligeti, Phys. Lett. **B364**, 75 (1995).

[8] S. Titard and F. Yndurain, Phys. Rev. **D49**, 6007 (1994); Phys. Rev. **D51**, 6348 (1995).

[9] A. Pineda and F. Ynduráin, Phys. Rev. **D58**, 094022 (1998); **D61**, 077505 (2000).

[10] K. Melnikov and A. Yelkhovsky, Phys. Rev. **D59**, 114009 (1999).

[11] N. Brambilla and A. Vairo, Phys. Rev. **D62**, 094019 (2000).

[12] A. Hoang, M. Smith, T. Stelzer and S. Willenbrock, Phys. Rev. **D59**, 114014 (1999).

[13] M. Beneke, Phys. Lett. **B434**, 115 (1998).

[14] A. Penin and A. Pivovarov, Phys. Lett. **B435**, 413 (1998).

[15] A. Hoang, Phys. Rev. **D61**, 034005 (2000); M. Beneke and A. Signer, Phys. Lett. **B471**, 233 (1999).

[16] N. Brambilla, Y. Sumino and A. Vairo, Phys. Lett **B513**, 381 (2001).

[17] Y. Sumino, hep-ph/0104259.

[18] A. Pineda, JHEP **0106**, 022 (2001).

[19] N. Brambilla, Y. Sumino and A. Vairo, hep-ph/0108084.

[20] K. Melnikov and T. v. Ritbergen, Phys. Lett. **B482**, 99 (2000).

[21] K. Chetyrkin and M. Steinhauser, Phys. Rev. Lett. **83**, 4001 (1999); Nucl. Phys. **B573**, 617 (2000).

[22] N. Gray, D. J. Broadhurst, W. Grafe and K. Schilcher, Z. Phys. **C48**, 673 (1990).

[23] S. Larin, T. v. Ritbergen and J. Vermaseren, Nucl. Phys. **B438**, 278 (1995).

[24] D. E. Groom et al., Eur. Phys. Jour. **C15**, 1 (2000).

[25] E. Eichten, K. Gottfried, T. Kinoshita, K. Lane and T. Yan, Phys. Rev. **D17**, 3090 (1978); **D21**, 313(E) (1980); **D21**, 203 (1980).

[26] A. Martin, Phys. Lett. **93B**, 338 (1980).

[27] C. Quigg and J. Rosner, Phys. Lett. **71B**, 153 (1977).

[28] M. Eidemüller and M. Jamin, Phys. Lett. **B498**, 203 (2001).